

STRUCTURAL AND MAGNETIC PROPERTIES OF $Gd_{1-x}Bi_xFeO_3$

 L.M. Ramírez Guzmán*,  J.A. Gómez Cuaspud,  C.A. Parra Vargas

Grupo Fisica de Materiales (GFM), Universidad Pedagógica y Tecnológica de Colombia,
Tunja, Colombia

Abstract. This work presents the synthesis of the $Gd_{1-x}Bi_xFeO_3$ system by the combustion method at a temperature of 650°C using citric acid, the doping with Bi^{3+} took values from $x=0.0$ to $x=0.14$ with an increase of 0.02 per sample. The structural characterization of the system was carried out with the application of X-Ray Diffraction (XRD), which by Rietveld refinement showed a perovskite-type compound with orthorhombic structure, *Pbnm* space group, preferential orientation in the (112) plane and no secondary phases. The micrographs SEM show the presence of particles with irregular shape and average particle size between 0.092 to 0.24 μm . Finally, the magnetic analysis showed that the materials obtained exhibit anti-ferromagnetic properties with ferromagnetic components.

Keywords: *Combustion method, ferromagnetism, orthoferrites, X-ray diffraction patterns.*

***Corresponding Author:** Laura Milena Ramírez Guzmán, Grupo Fisica de Materiales (GFM), Universidad Pedagógica y Tecnológica de Colombia, Tunja, Colombia,
e-mail: laura.ramirez01@uptc.edu.co

Received: 13 September 2024;

Accepted: 4 October 2024;

Published: 16 October 2024.

1. Introduction

Rare earth orthoferrites with general formula $RFeO_3$ (where R is a rare earth element) have been the subject of study, due to its unique structural, electrical, magnetic properties at low temperature and interesting dielectric properties over a wide temperature range (Nakhaei & Khoshnoud, 2019). These properties make rare earth orthoferrites potential candidates for applications in fuel cells, magneto-optical devices, catalysis, sensors (Cao *et al.*, 2018), storage devices etc. Orthoferrites possess a perovskite-like, orthorhombic structure with *Pbnm* space group, which magnetic properties arise from the different magnetic transitions of Fe^{3+} and R^{3+} ions (Katba *et al.*, 2019). Within these transitions, the related with the Neel temperature at 5K and between 600 - 700 K (Xue *et al.*, 2019), spin reorientation temperatures between 170 to 480 K (Fatema *et al.*, 2024) and some additional, can present a weak ferromagnetic behavior caused by Dzyaloshinskii-Moriya interaction (DM), attributed to the antisymmetric Fe^{3+} - Fe^{3+} exchange (Nakhaei & Khoshnoud, 2021).

Manipulation of synthesis methods, doping and rare earth assignment result in emerging behaviors such as ferroelectricity and altered magnetic behavior in orthoferrites, which is associated with the ionic radius that influences the crystal structure and is closely related to the Néel temperature (Zhou *et al.*, 2014). In addition to several

How to cite (APA):

Ramírez, L.M., Gómez, J.A. & Parra, C.A. (2024). Structural and magnetic properties of $Gd_{1-x}Bi_xFeO_3$. *Advanced Physical Research*, 6(3), 159-165 <https://doi.org/10.62476/apr63159>

interesting magnetic properties, some orthoferrites are recognized in the literature is multiferroic even at room temperature (Lee *et al.*, 2011).

Although their functionality is limited due to low magnetization and high dielectric loss, the unique physical properties of perovskites are important for various technological applications. Normally, these oxides are synthesized by the solid-state reaction method, however, the presence of secondary phases generated by this method due to the low-homogeneity, which leads to thermal treatments with intermediate grinding, has promoted the development of new methods with higher efficiency, in which stand out: the sol-gel, hydrothermal and combustion methods (Coutinho *et al.*, 2017), among which the latter is highlighted as it is more economical and favors the obtaining of purer materials (Wu *et al.*, 2014). The objective of this work is to perform the synthesis of a system based on $\text{Gd}_{1-x}\text{Bi}_x\text{FeO}_3$ composition (x varies between 0 and 0.14) by the combustion method, where the substitution is performed by Bi^{3+} ions to enhance the system, taking into account that bismuth is a larger ion and promote the distortion the structure, modifying the magnetic behavior of the material and possibly inducing ferroelectricity (Fatema *et al.*, 2024).

2. Material and Methods

Polycrystalline $\text{Gd}_{1-x}\text{Bi}_x\text{FeO}_3$ were synthesized by the combustion method. Stoichiometric amounts of the nitrates (previously titrated) were taken and dissolved under magnetic stirring and temperature control. Subsequently, citric acid was added in a ratio of 1:0.5 mol: mol, in relation to the total content of metal cations. The solution was kept at a constant temperature of 80°C for 2 h, then treated at 200°C until evaporation of the solvent and consolidation of a gel. This was heated to 300°C for the combustion reaction. Finally, the powders obtained were milled and calcinated at 650°C for 18 h.

The obtained powders were determined using a X-ray powder diffractometer (PANalytical X'pert PRO-MD with Bragg-Brentano configuration), using the Cu-K α radiation ($\lambda = 1.5418 \text{ \AA}$) at the range of $2\theta \approx 20 - 90^\circ$. The structural parameters were obtained from the Rietveld refinement analysis performed using the GSAS software (Rosales *et al.*, 2020). The morphological properties were examined using scanning electron microscopy (SEM) in a JSM 6490-LV JEOL electron microscope and the elemental analysis (EDS). The magnetic behavior, temperature-dependent and field-dependent measurements were performed in a vibrating sample magnetometer (VersaLab VSM, Quantum Design) under external magnetic fields ranging from -30 and 30 kOe and temperatures between 50 and 370 K in Zero-Field-Cooled / Field-Cooled modes (ZFC/FC).

3. Results and Discussion

Figure 1a shows the XRD patterns for each of the $\text{Gd}_{1-x}\text{Bi}_x\text{FeO}_3$ compounds ($x = 0.0, 0.02, 0.04, 0.06, 0.08, 0.10, 0.12, 0.14$), refined by the Rietveld method. The analysis determined that the materials present an orthorhombic structure with $Pbnm$ space group (62), with preferential orientation along the (112) facet, without the presence of additional peaks that evidence secondary phases, additionally no significant displacements are visualized as the Bi content increases, nor broadening since the substitutions are at low percentages. The variation of the lattice parameters obtained from the refinement as a function of the bismuth content is shown in Figure 1b, a small increase in the parameters

and cell volume is observed as the bismuth content increases. This behavior can be attributed to the deformation of the unit cell due to the substitution of the Gd^{3+} ion by the Bi^{3+} ion, because the ionic radius of Bi^{3+} is larger than Gd^{3+} ion (Li *et al.*, 2010; Rosales *et al.*, 2020). For the $GdFeO_3$ sample, the cell parameters are $a = 5.34 \text{ \AA}$, $b = 5.60 \text{ \AA}$ and $c = 7.66 \text{ \AA}$, similar to those reported by Sudandararaj *et al.* (2019) obtained by co-precipitation method and by Panchwanee *et al.* (2017) in their synthesis method by solid-state reaction. The modification of the unit cell likewise produced changes in the Fe-O-Fe bond angles, affecting the spin arrangement and thus the super-exchange interaction (Shah *et al.*, 2012).

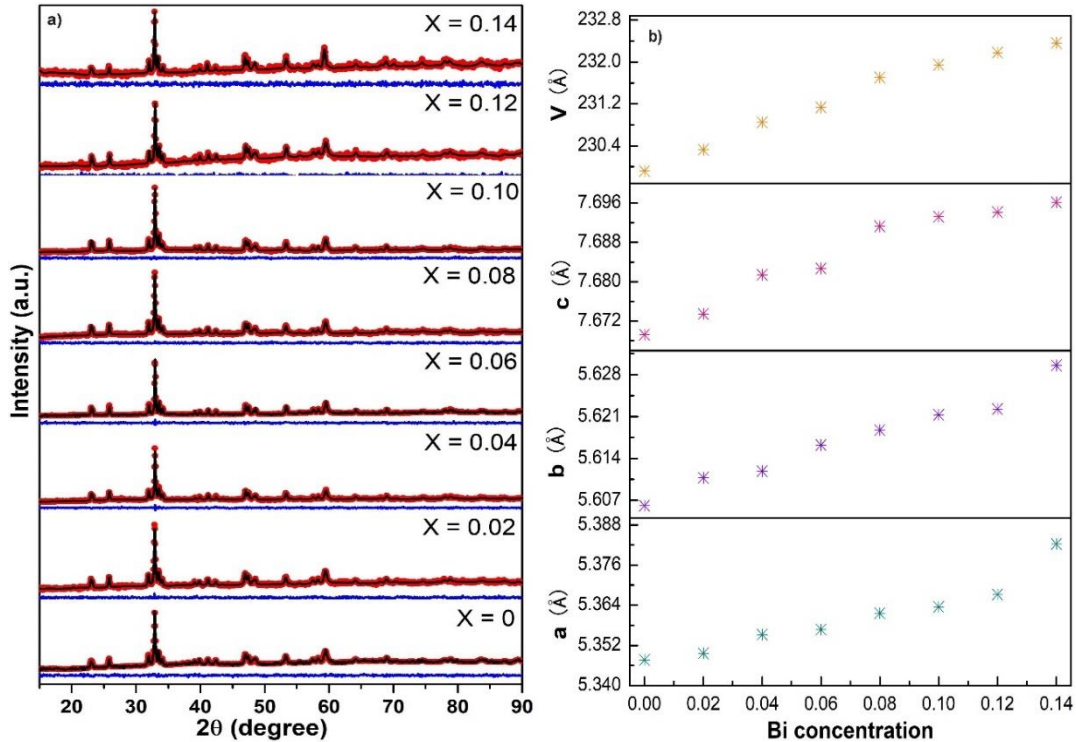


Figure 1. a) XRD pattern of $Gd_{1-x}Bi_xFeO_3$ fitted with the Rietveld refinement
b) Variation of the lattice parameters vs Bi^{3+} concentration

In the SEM images (see Figure 2), an irregular morphology is observed with well-defined grains and more homogeneous distribution at low doping levels. At high Bi^{3+} contents, the grains are more irregular with the presence of agglomerations, made up of particles of different sizes. The sample with doping $x = 0.14$ in its morphology presents grains with poorly defined boundaries and high porosity, which may influence the magnetic properties of this material. The average diameter is in the range of $0.092 - 0.124 \mu\text{m}$, comparable to those obtained by Ma *et al.* (2023), in Bi-modified Gd orthoferrites synthesized by the sol-gel method at 700°C .

SEM images demonstrate the effect of Bi concentration in $GdFeO_3$ on grain size. It is observed that as the Bi content increases the grain size increases, indicating that bismuth possibly accelerates the grain growth rate and helps the formation of oxygen vacancies, due to its volatility, as observed in research related to the $BiFeO_3$ compound (Padmasree *et al.*, 2021; Zhang *et al.*, 2024). The chemical composition of the samples examined through EDX analysis are shown in Figure 4. The characteristic peaks

of Gd, Bi, Fe and O are observed, which indicate the degree of purity of the materials. In addition, there are peaks characteristic of C, as a consequence of the synthesis by the combustion method. The results wt% and at% are inserted in the spectra. The at% found is equivalent to the stoichiometry of the materials, further increasing the Bi content and decreasing the Gd content.

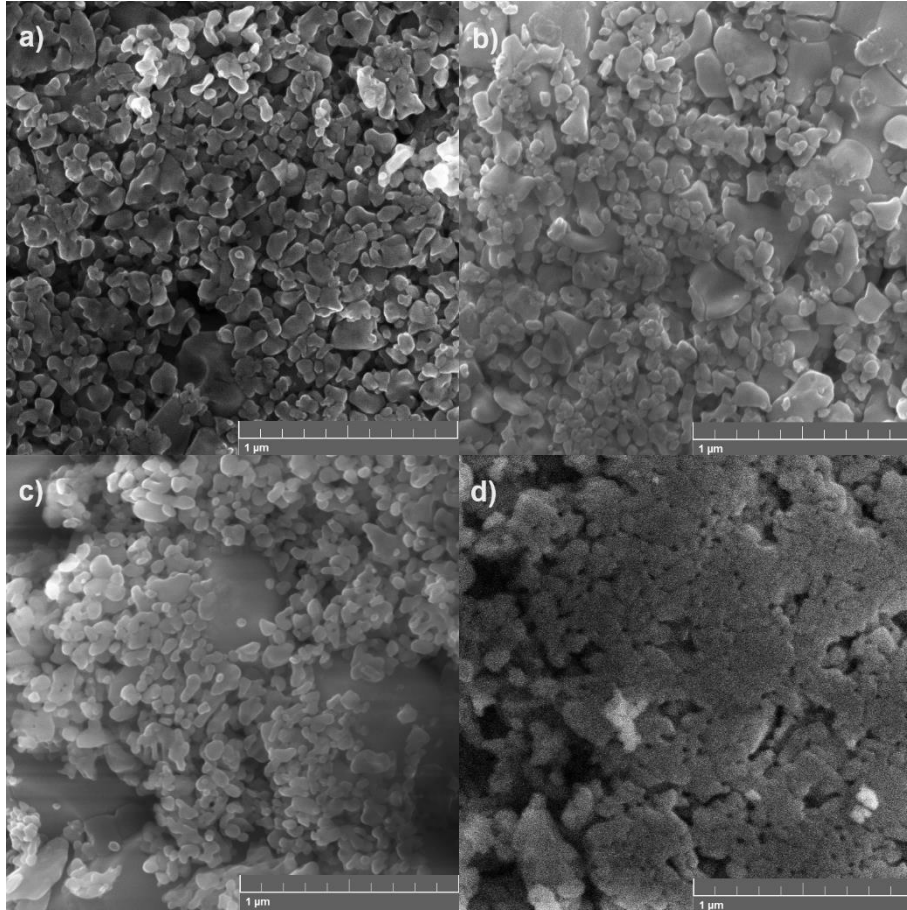


Figure 2. Images SEM for $Gd_{1-x}Bi_xFeO_3$ system with a) $x=0.0$, b) $x=0.06$, c) $x=0.10$ y d) $x=0.14$

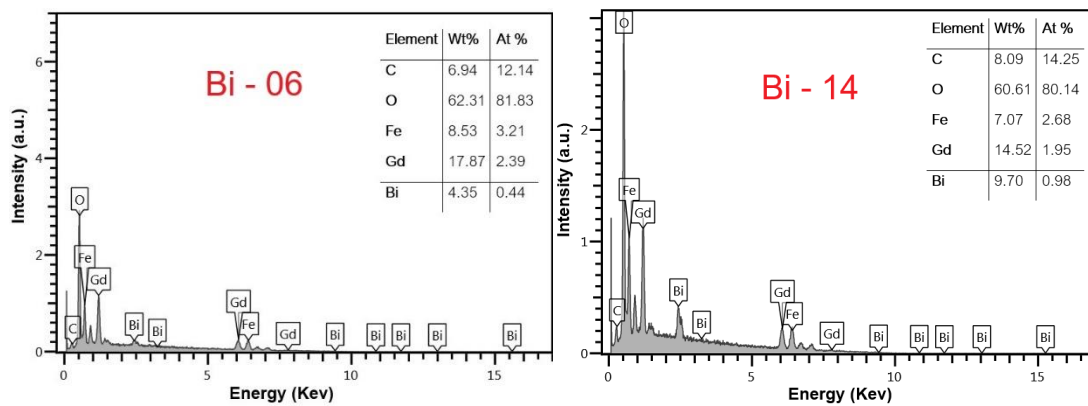


Figure 3. EDX spectra with atomic percentaje of Bi – 06 and Bi – 14

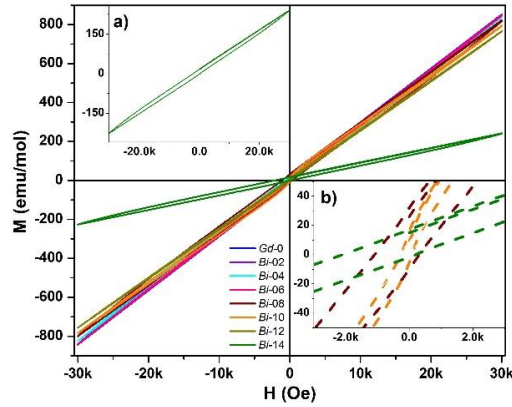


Figure 4. M-H curves measured at 300 K a for $Gd_{1-x}Bi_xFeO_3$ compounds. Insets: a) hysteresis curve for $x = 0.14$ and b) magnification of the hysteresis loops

The figure 4 shows the magnetization vs magnetic field (M-H) at 300 K. The materials show a linear hysteresis characteristic of an antiferromagnetic behavior with slight ferromagnetic components, which cause a thin hysteresis cycle (See Figure 4b). The materials show high magnetization values except for the sample $Gd_{0.86}Bi_{0.14}FeO_3$, which decreased drastically, however, this material presents the highest values of remanent magnetization (M_r) and coercive field (H_c), as shown in Table 1. This behavior is due to a tilted spin structure, which can be attributed to the presence of the Bi^{3+} ion occupying the Gd^{3+} site, which has been reported in other investigations carried out by Ogunniran et al. (2019) in substitutions with 10% Bi, which improved the exchange interactions between the different magnetic sublattices, being a weakly ferromagnetic ion.

Table 1. Magnetic parameters for $Gd_{1-x}Bi_xFeO_3$ obtained at 300 K

Sample	Gd-0	Bi-02	Bi-04	Bi-06	Bi-08	Bi-10	Bi-12	Bi-14
M_r (emu/mol)	16.74	19.37	19.47	8.02	31.93	13.23	8.51	17.06
H_c (Oe)	335.20	285.95	169.86	53.48	704.31	83.69	167.75	1148.23

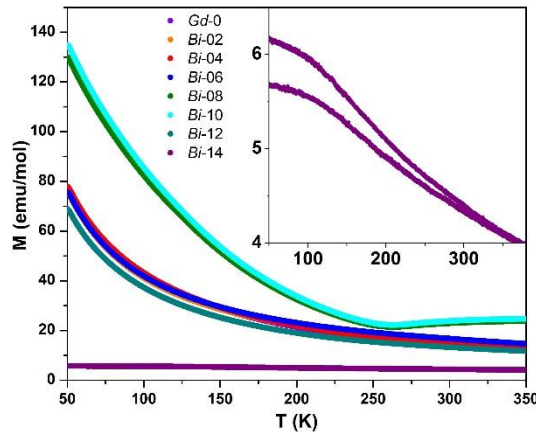


Figure 5. Magnetization curve as a function of field at ambient temperature of the $Gd_{1-x}Bi_xFeO_3$ system. Inset: ZFC - FC curve for material with 14% of Bi

The dependence of the magnetization as a function of temperature at a field of 500 Oe is shown in Figure 5. For materials with $x = 0$ up to $x = 0.12$, the ZFC - FC curves overlap and the magnetization increases rapidly as the temperature decreases, around 250

to 300 K there is a slight separation of the curves indicating a weak ferromagnetic behavior at temperatures close to ambient, highlighting the samples with compositions of 8% and 10% Bi by presenting high magnetization values and an inflection around ~250 K, which is associated with a spin reorientation temperature between Gd^{3+} and Fe^{3+} ions characteristic of these orthoferrites (Khan *et al.*, 2020) and which has been reported by Panchwatee *et al.* (2018) in Mn-modified $GdFeO_3$. The sample with $x = 0.14$ (inset), the magnetization presents the same behavior as the other materials, however, the magnetization is low with a value of 5.7 emu/mol and a more evident bifurcation than the other materials is observed from ~280 K onwards.

The variation of the magnetization as a function of temperature allowed us to visualize that at low temperatures the magnetization is high, because the rare earth moments are parallel to the net Fe momentum (Vilarinho *et al.*, 2022; Zhou *et al.*, 2014). The super-exchange interactions between Fe ions, contribute to an antiferromagnetic coupling along one crystallographic direction and the low structure symmetry causes a tilted spin structure giving rise to weak ferromagnetism in another crystallographic direction. The magnetic properties of these materials, therefore, are strongly correlated with the nature and concentration of the dopant ion, the Fe-O-Fe bond angles, the synthesis method and the morphology (Ahmed *et al.*, 2015).

4. Conclusion

The $Gd_{1-x}Bi_xFeO_3$ compounds synthesized by the combustion method presented an orthorhombic structure, without the presence of secondary phases. The doping with Bi permit modified the lattice parameters and the cell volume, due to the deformation of the unit cell caused by this ion, which significantly modified the size and shape of the grains, since the higher the bismuth concentration, more irregularity the grains and correspondingly tend to be more agglomerated.

The modifications in the structure and morphology in these materials led to an antiferromagnetic behavior with mild ferromagnetic components. Additionally, this study highlights the complexity of the magnetic interactions in these materials, underlining the importance of considering several factors to fully understand their behavior.

References

- Ahmed, M.A., Azab, A.A. & El-Khawas, E.H. (2015). Structural, magnetic and electrical properties of Bi doped $LaFeO_3$ nano-crystals, synthesized by auto-combustion method. *Journal of Materials Science: Materials in Electronics*, 26, 8765-8773.
- Cao, E., Chu, Z., Wang, H., Hao, W., Sun, L. & Zhang, Y. (2018). Effect of film thickness on the electrical and ethanol sensing characteristics of $LaFeO_3$ nanoparticle-based thick film sensors. *Ceramics International*, 44(6), 7180-7185.
- Coutinho, P.V., Cunha, F. & Barrozo, P. (2017). Structural, vibrational and magnetic properties of the orthoferrites $LaFeO_3$ and $YFeO_3$: A comparative study. *Solid State Communications*, 252, 59-63.
- Dhara, A., Sain, S., Maji, P., Das, S. & Pradhan, S.K. (2019). Dielectric relaxation, AC conductivity behavior and its relation to microstructure in mechanochemically synthesized Mn-doped CeO_2 nanocrystals. *Solid State Sciences*, 87, 93-100.
- Fatema, M., Mala, N.A., Qahtan, A.A., Manzoor, S., Somvanshi, A., Mahboob, H. & Husain, S. (2024). Structural analysis, ferroic properties with enhanced magnetoelectric coupling in novel $(1-x)BiFeO_3-(x)GdFeO_3$ nanocomposites. *Journal of Alloys and Compounds*, 976, 173268.

- Katba, S., Jethva, S., Panchal, G., Choudhary, R.J., Phase, D.M. & Kuberkar, D.G. (2019). Studies on electronic structure and dielectric properties of La-doped ErFeO₃ orthoferrites. *Journal of Alloys and Compounds*, 789, 814-824.
- Khan, A.A., Ahlawat, A., Deshmukh, P., Dileep, D., Singh, R., Karnal, A.K. & Satapathy, S. (2020). Effect of Sm doping on structure, dielectric and magnetic properties of GdFeO₃. *Ceramics International*, 46(12), 19682-19690.
- Lee, J.H., Jeong, Y.K., Park, J.H., Oak, M.A., Jang, H.M., Son, J.Y. & Scott, J.F. (2011). Spin-canting-induced improper ferroelectricity and spontaneous magnetization reversal in SmFeO₃. *Physical Review Letters*, 107(11), 117201.
- Li, J.B., Rao, G.H., Xiao, Y., Liang, J.K., Luo, J., Liu, G.Y. & Chen, J.R. (2010). Structural evolution and physical properties of Bi_{1-x}Gd_xFeO₃ ceramics. *Acta Materialia*, 58(10), 3701-3708.
- Ma, Y., Shen, H., Fang, Y., Geng, H., Zhao, Y., Li, Y. & Ma, Y. (2023). Effect of bismuth on the structure, magnetic and photocatalytic characteristics of GdFeO₃. *Magnetochemistry*, 9(2), 45.
- Nakhaei, M., Khoshnoud, D.S. (2019). Influence of particle size and lattice distortion on magnetic and dielectric properties of NdFeO₃ orthoferrite. *Physica B: Condensed Matter*, 553, 53-58.
- Nakhaei, M., Khoshnoud, D.S. (2021). Study on structural, magnetic and electrical properties of ReFeO₃ (Re= La, Pr, Nd, Sm & Gd) orthoferrites. *Physica B: Condensed Matter*, 612, 412899.
- Padmasree, G., Kumar, S., Kumar, N., Reddy, P. & Reddy, G. (2021). Structural and magnetic properties of Y_{1-x}Dy_xFeO₃ multiferroics. *Materials Today: Proceedings*, 46(6), 2201-2204.
- Panchwatee, A., Raghavendra, V., Gupta, A. & Sathe, V.G. (2017). Study of spin-phonon coupling and magnetic field induced spin reorientation in polycrystalline multiferroic GdFeO₃. *Materials Chemistry and Physics*, 196, 205-212.
- Panchwatee, A., Reddy, V., Gupta, A., Bharathi, A. & Phase, D.M. (2018). Study of local distortion and spin reorientation in polycrystalline Mn doped GdFeO₃. *Journal of Alloys and Compounds*, 745, 810-816.
- Rosales, O., Sánchez, F., Camacho, M.A., Cortés, C.A. & Bolarín, A.M. (2020). Synthesis of magnetically removable photocatalyst based on bismuth doped YFeO₃. *Materials Science and Engineering: B*, 261, 114773.
- Shah, J., Kotnala, R.K. (2012). Room temperature magnetoelectric coupling enhancement in Mg-substituted polycrystalline GdFeO₃. *Scripta Materialia*, 67, 316-319.
- Sudandararaj, A.T., Kumar, G.S., Dhivya, M., Eithiraj, R.D. & Banu. I.B. (2019). Band structure calculation and rietveld refinement of nanoscale GdFeO₃ with affirmation of Jahn Teller's distortion on electric and magnetic properties. *Journal of Alloys and Compounds*, 783, 393-398.
- Vilarinho, R., Weber, M.C., Guennou, M., Miranda, A.C., Dias, C., Tavares, P., Kreisel, J., Almeida, A. & Agostinho, J. (2022). Magnetostructural coupling in RFeO₃ (R = Nd, Tb, Eu and Gd). *Scientific Reports*, 12, 9697.
- Wu, A., Wang, Z., Wang, B., Ban, X., Jiang, L., Xu, J., Yuan, S. & Cao, S. (2014). Crystal growth and magnetic properties of GdFeO₃ crystals by floating zone method. *Solid State Communications*, 185, 14-17.
- Xue, F., Tian, Y., Guo, F., Qiu, L., Wang, W. & Tang, W. (2023). Structural, dielectric and impedance properties of BiFeO₃-GdFeO₃ ceramics. *Materials Chemistry and Physics*, 301, 127675.
- Zhang, M.H., Tan, Y., Yang, T. & Chen, L.Q. (2024). Influence of oxygen vacancies on the domain wall stability in BiFeO₃. *Journal of the American Ceramic Society*, 1-7.
- Zhou, Z., Guo, L., Yang, H., Liu, Q. & Ye, F. (2014). Hydrothermal synthesis and magnetic properties of multiferroic rare-earth orthoferrites. *Journal of Alloys and Compounds*, 583, 21-31.